AIAA 80-0362R

Effect of Mach Number on Slender Vehicle Dynamics

Lars E. Ericsson*
Lockheed Missiles & Space Company, Inc., Sunnyvale, Calif.

An analytic method has been developed for fast computation of the longitudinal unsteady aerodynamics of slender axisymmetric bodies. The method is anchored by two well-established theories; the embedded Newtonian theory for hypersonic speeds and the slender body theory for sonic speed. The computed pitch damping is in good-to-excellent agreement with available experimental data, and the analytic method should serve well in the preliminary design of tactical and ballistic missiles.

Nomenclature

C_{mq} $= \dfrac{\partial C_m}{\partial(cq/U_\infty)}$

$C_{N\alpha}$ $= \dfrac{\partial C_N}{\partial \alpha}$

$C_{m\dot{\alpha}}$ $= \dfrac{\partial C_m}{\partial(c\dot{\alpha}/U_\infty)}$

C_γ = parameter defined in Eq. (4)
c = reference length $(c=d_B)$
d = body diameter
l = total body length (see Fig. 1)
l_0 = sharp-cone length
M = Mach number
M_∞^* = minimum Newtonian Mach number
M_p = pitching moment: coefficient $C_m = M_p/(\rho_\infty U_\infty^2/2)Sc$
N = normal force: coefficient $C_N = N(\rho_\infty U_\infty^2/2)S$
p = static pressure: coefficient $C_p = (p-p_\infty)/(\rho_\infty U_\infty^2/2)$
q = pitch rate
Re = Reynolds number, $Re_{l\infty} = lU_\infty/v_\infty$
S = reference area $=\pi c^2/4$
t = time
U = axial velocity
$V_\perp$ = velocity component normal to body surface
x = axial distance from nosetip (see Fig. 1).
α = angle of attack (see Fig. 1).
$\dot{\alpha}$ $= \dfrac{\partial \alpha}{\partial t}$
β = Prandtl-Glauert compressibility parameter $= \sqrt{1-M_\infty^2}$
γ = ratio of specific heats = 1.4 for air
θ_c = cone half-angle
v = kinematic viscosity of air
ρ = air density
φ = azimuth (see Fig. 1)

Subscripts

B = base
CG = center of gravity or oscillation center
eff = effective
Newt = Newtonian theory
TC = tangent cone
SB = slender body
∞ = freestream value

Introduction

A FAST computational method is needed to determine the unsteady aerodynamics of tactical weapons with sufficient accuracy for preliminary design. The present paper presents results of a recently completed study[1] aimed at improving the accuracy of existing rapid computational technology[2] for prediction of slender vehicle pitch damping.

The method developed in this paper is anchored by two well-established theories: the Newtonian theory for hypersonic speeds and the slender body theory for sonic speed. An analytic theory already exists[3,4] for the computation of nose bluntness effects on hypersonic vehicle dynamics. In the present paper, simple means are derived, by use of the tangent-cone approach, whereby the sharp-cone hypersonic aerodynamics can be corrected for γ-effects to agree with Method of Characteristics (MOC) results. A similar tangent-wedge approach was used in Ref. 5 to get Newtonian airfoil aerodynamics to agree with MOC results. In this manner, slender vehicle pitch damping can be computed down to moderate supersonic Mach numbers.

At subsonic speeds, the analytic approach used earlier to develop rapid computational means for determination of slender wing dynamics[6,7] is applied to slender body geometries. As the delta wing formed the basis for the slender wing theory,[6,7] so the cone forms the basis for the slender vehicle analysis. The experimentally measured $C_{N\alpha}$-variation with Mach number, corrected for support interference effects,[8] supplies the means for correcting slender body theory[9] for Mach number effects.

Analysis

Two theories have been of great help for the vehicle designer in the past; slender body theory[9] and Newtonian theory.[10] For present day design, however, these simple theories have proven inadequate because they cannot correctly account for the effects of Mach number and nose bluntness. The analytic method described in Refs. 3 and 4 predicts the change in sharp-cone damping due to nose bluntness effects. Before the blunted- (and sharp-) cone characteristics can be determined, knowledge of the sharp-cone dynamic characteristics is necessary. They could be obtained through numerical methods,[11] but that would destroy the simplicity sought here for preliminary design. The Newtonian method is valid only in the limiting case of $\gamma \rightarrow 1$. Reference 5 shows how to use the tangent-wedge method to correct the Newtonian method for γ-effects to make it agree with MOC computations. For the cone, one can use a similar approach (the tangent-cone method) to define the γ-correction, as inviscid

Presented as Paper 80-0362 at the AIAA 18th Aerospace Sciences Meeting, Pasadena, Calif., Jan. 14-16, 1980; submitted Jan. 18, 1980; revision received May 9, 1980.

*Senior Consulting Engineer. Associate Fellow AIAA.

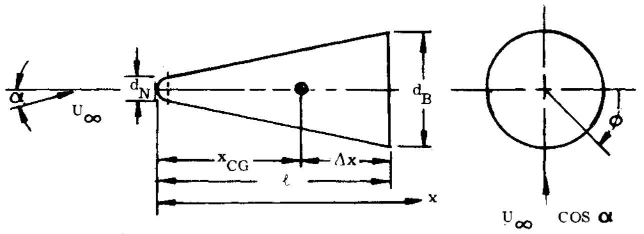

Fig. 1 Definition of coordinates and parameters.

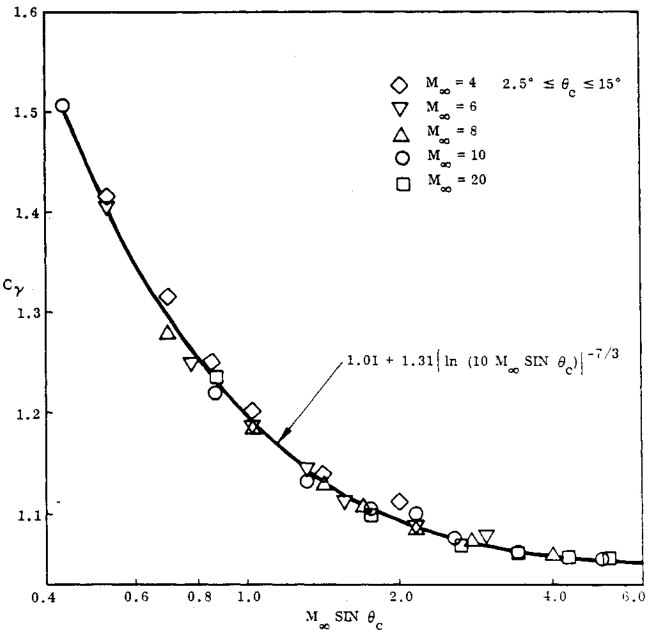

Fig. 2 Gamma-correction of Newtonian characteristics.

crossflow effects usually can be neglected at the supersonic and hypersonic speeds considered here, i.e., $M_\infty > M^*_\infty$.

Gamma-Corrected Newtonian Theory

In the Newtonian formulation, the inviscid flow cone pressure coefficient is (see Fig. 1 for definition)

$$(C_p)_{\rm Newt} = 2(V_\perp / U)^2 \tag{1}$$

$$V_\perp / U = \cos\alpha\sin\theta_c + \sin\alpha\cos\theta_c\sin\varphi \tag{2}$$

Comparing the results of Eq. (1) with those of MOC[12] for $\alpha = 0$ defines a pressure coefficient ratio $C_\gamma = (C_P)_{TC}/(C_p)_{\rm Newt}$, which is dependent only upon the hypersonic similarity parameter $M_\infty \sin\theta_c$ for cone angles in the range of interest, 2.5 deg $\leq \theta_c \leq$ 15 deg (see Fig. 2). The results in Fig. 2 give the following modification of Eq. (1), valid for $M_\infty \geq M^*_\infty$†:

$$(C_p)_{TC} = C_\gamma \, C_{p\rm Newt}$$

$$C_\gamma = 1.01 + 1.31[\ln(10\,M_\infty \sin\theta_c)]^{-7/3} \tag{3}$$

For oscillations around x_{CG} with the angular rate q rad/s, the expression for $V_\perp / U$ is as follows:

$$\frac{V_\perp}{U} = \cos\alpha\sin\theta_c + \sin\alpha\cos\theta_c\sin\varphi + \frac{(x - x_{CG} + r\tan\theta_c)q}{U_\infty}\cos\theta_c\sin\varphi \tag{4}$$

†The critical Mach number M^*_∞ is defined as $M^*_\infty = 0.4\csc\theta_c$ for a cone.

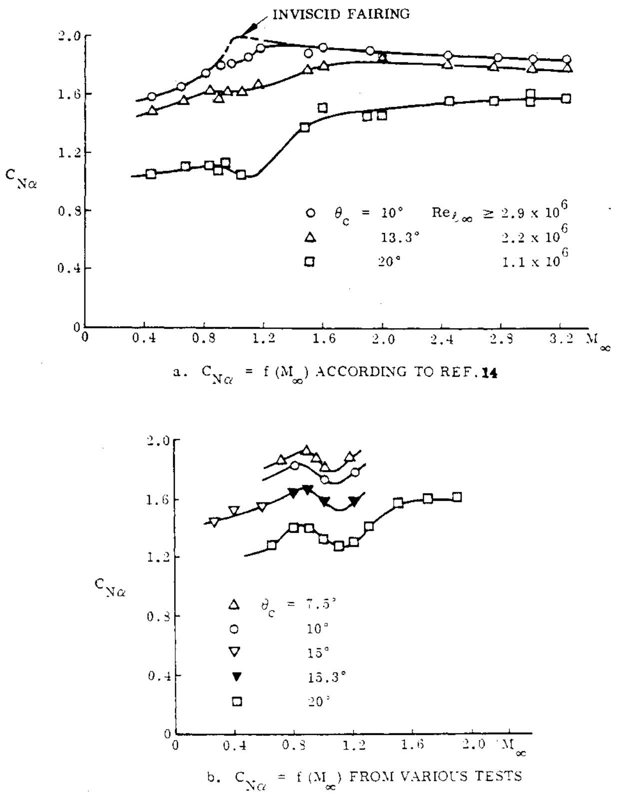

Fig. 3 $C_{N\alpha}$ as a function of Mach number for various cones.

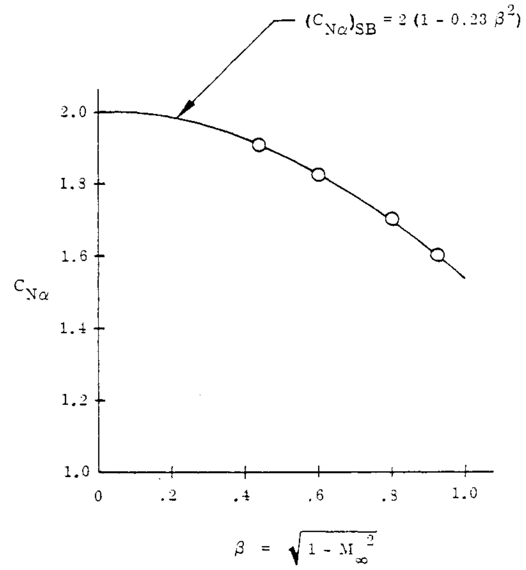

Fig. 4 Slender cone $C_{N\alpha} = f(\beta)$.

Equations (1-4) define the following sharp-cone stability derivatives:

$$C_{m\alpha} = -C_\gamma\left[\left(\frac{2}{3} - \frac{x_{CG}}{l_0}\right)\cot\theta_c + \tan\theta_c\right] \tag{5}$$

$$C_{mq} = -\frac{C_\gamma}{4\tan^2\theta_c}\left[\left(1 + \tan^2\theta_c - \frac{4}{3}\frac{x_{CG}}{l_0}\right)^2 + \frac{2}{9}\left(\frac{x_{CG}}{l_0}\right)^2\right]$$

Modified Slender Body Theory

In Ref. 6, it was shown how the slender wing theory[13] could be modified to be valid at subsonic Mach numbers down to incompressible flow, $0 \leq M_\infty \leq 1$. An equivalent delta wing was defined which gave the correct normal force derivative $(C_{N\alpha})$ at $\alpha = 0$. To this equivalent delta wing, for which the

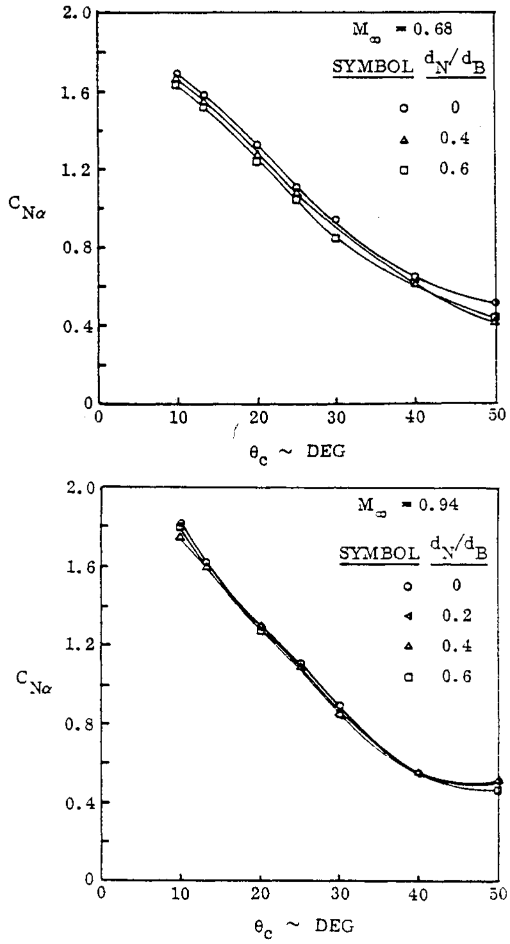

Fig. 5 Effect of nose bluntness on cone $C_{N\alpha}$.

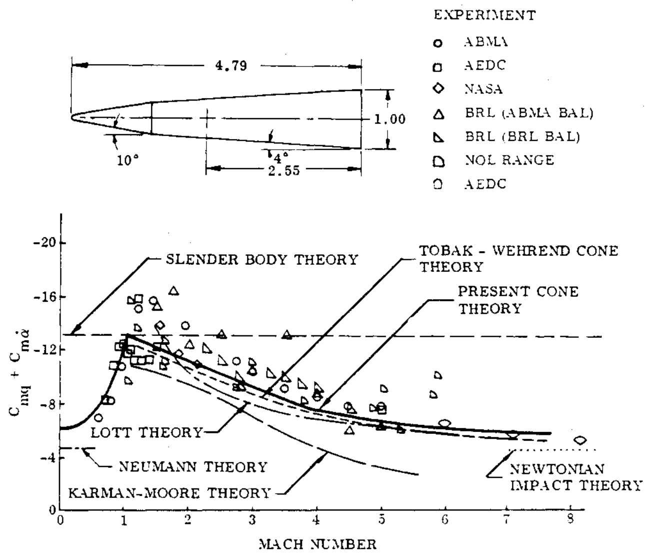

Fig. 6 Comparison between theoretical predictions and experimental results for pitch damping of a slender vehicle.

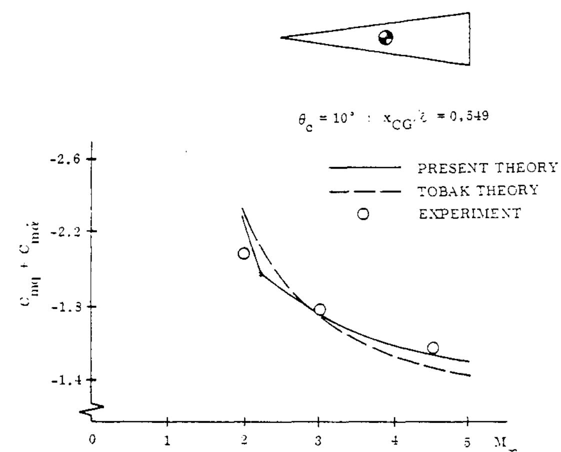

Fig. 7 Predicted and measured damping of a 10-deg sharp cone.

trailing edge moved forward with decreasing Mach number, the slender wing formulation was applied. The dynamic slender wing characteristics obtained in this manner agree well with available experimental results and with predictions obtained through more complicated theories (see Ref. 6). It is natural, of course, to try a similar approach for prediction of slender-cone dynamics at subsonic speeds.

The normal force derivative $C_{N\alpha}$ measured on slender sharp cones[14-17] is shown in Fig. 3. Except for a peculiar breakaway near sonic speed, the data show the expected continuing increase of $C_{N\alpha}$ with increasing subsonic Mach number. It can be shown that the breakaway is caused by sting interference effects that are amplified through boundary layer transition occurring on the aft body near the base.[8] Correcting for this anomaly, as shown, gives the slender cone $C_{N\alpha}$-variation displayed in Fig. 4. The Mach number effect can be expressed as follows:

$$(C_{N\alpha})_{SB} = 2(1-0.23\beta^2) = 2(0.77+0.23\,M_\infty^2) \quad (6)$$

With $C_{N\alpha}$ determined in this manner, a direct application of the attached flow analysis of Ref. 6 defines the pitch damping derivative as follows:

$$C_{mq}+C_{m\dot\alpha} = -(C_{N\alpha})_{SB}\cos\alpha\,(l/c)^2\,(l_{\rm eff}/l - x_{CG}/l)^2 \quad (7)$$

$$l_{\rm eff}/l = \sqrt{0.77+0.23\,M_\infty^2} \quad (8)$$

Combining Eqs. (6-8) gives the following subsonic slender-cone damping:

$$C_{mq}+C_{m\dot\alpha} = -2(0.77+0.23\,M_\infty^2)\cos\alpha \times \left[(l/c)\sqrt{0.77+0.23\,M_\infty^2} - x_{CG}/c\right]^2 \quad (9)$$

According to the measurements in Ref. 14, Eq. (8) can be used also for blunted cones (see Fig. 5). In the present analysis Eq. (8) is, therefore, used for slender bodies of general shape.

Discussion of Results

The simple analytic predictions obtained are found to be in very good agreement with available experimental and theoretical results. In Fig. 6, the results are shown for a slender body geometry that has been used extensively in the past as a test for developed theories. The figure is Fig. 2 of Ref. 18 to which has been added the present results and those obtained by Lott.[19] Also added is the incompressible flow estimate obtained by in-house use of the Neumann theory.[20] The present computations, as well as those made by use of the Tobak-Wehrend theory,[21] are for a 6-deg equivalent cone.

It can be seen that the present approximate theory does as well as any of the other much more complex theories in predicting the experimental results, and it does it over the complete speed range of $0 \le M_\infty < \infty$. Figure 7 demonstrates that both the present theory and the Tobak-Wehrend theory[21] produce predictions that are in excellent agreement with the damping measured in free-flight (and consequently, without the sting interference problems discussed in Ref. 8) on a 10-deg sharp cone at supersonic Mach numbers.[22] The agreement is almost as good with the measured damping of a 12.5-deg sharp cone[23] after the experimental data have been corrected for sting interference (see Ref. 8 and Fig. 8).

A systematic investigation of slender cones of varying cone angle and nose bluntness[24] has provided a wealth of experimental data against which the present analytic method can be checked. Figure 9 shows that present predictions agree with the test results within the scatter of the experimental data. Note that the high-test Reynolds number eliminates the sting interference problem discussed in Ref. 8. Figure 9 demonstrates, therefore, that the present analytic method can predict the unsteady aerodynamics of sharp and blunted slender cones over the complete Mach number range of $0 \leq M_\infty < \infty$.

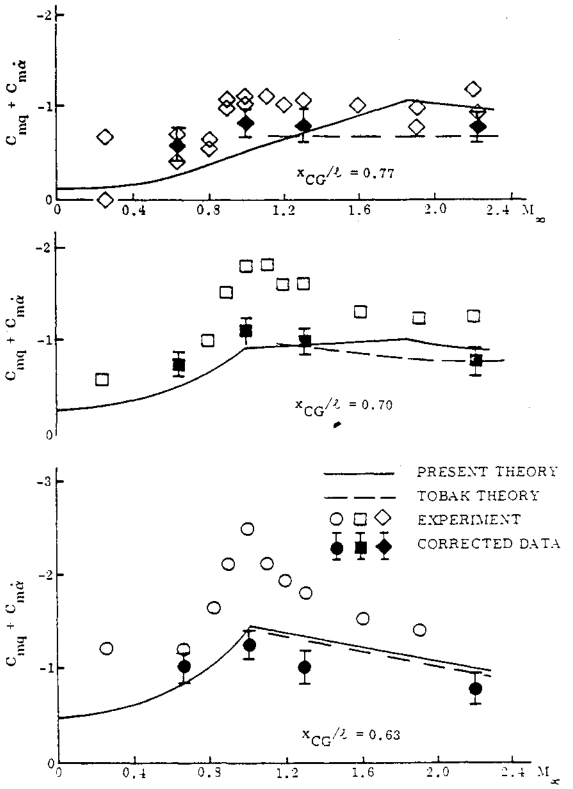

Fig. 8 Predicted and measured damping of a 12.5-deg sharp cone.

In Fig. 10, present predictions of ogive-cylinder dynamics are compared with experiment.[25] The agreement is rather good. At transonic and low supersonic speeds, the shoulder expansion and downstream shock-boundary layer interaction will have to be included for ogive- and cone-cylinder bodies. This can be done by extension of the analytic methods described in Refs. 26 and 27. However, this is beyond the scope of the present paper, and only the subsonic characteristics are predicted.

Figure 11 shows that present predictions are rather good also for cone-cylinders of considerable length,[28] at least at high subsonic speeds. The low Mach number trend of the experimental data is peculiar (compare Figs. 10 and 11). It has been shown recently[29] that the loads induced by asymmetric vortices on slender bodies at high angles of attack increase with increasing slenderness ratio and decrease with increasing Mach number, becoming of negligible magnitude at transonic

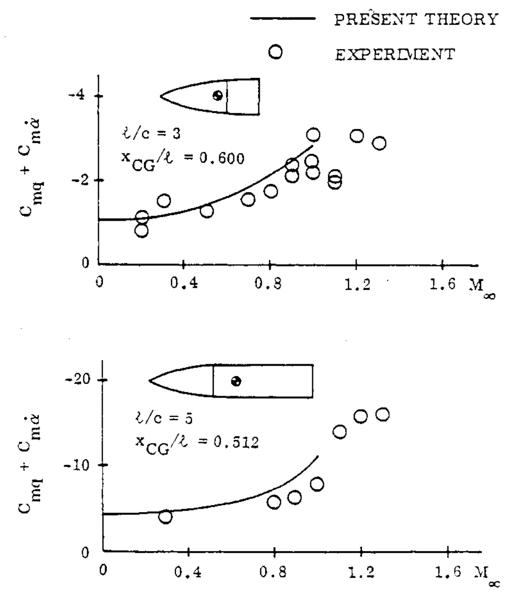

Fig. 10 Comparison between predicted and measured damping of ogive-cylinder bodies.

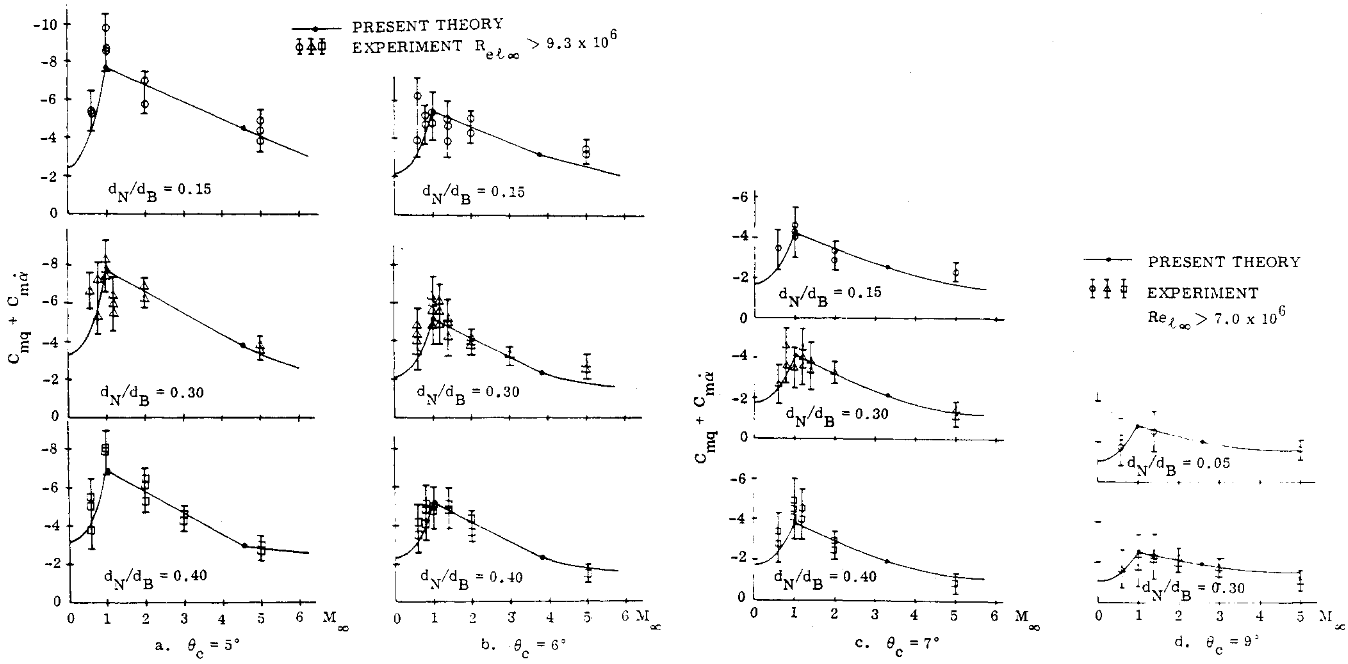

Fig. 9 Comparison between predicted and measured damping of a series of slender blunted cones.

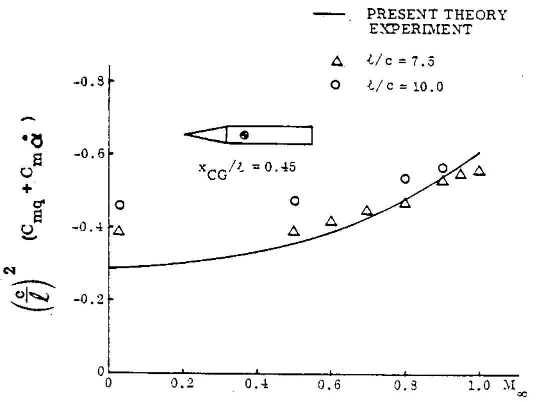

Fig. 11 Predicted and measured damping of cone-cylinder bodies.

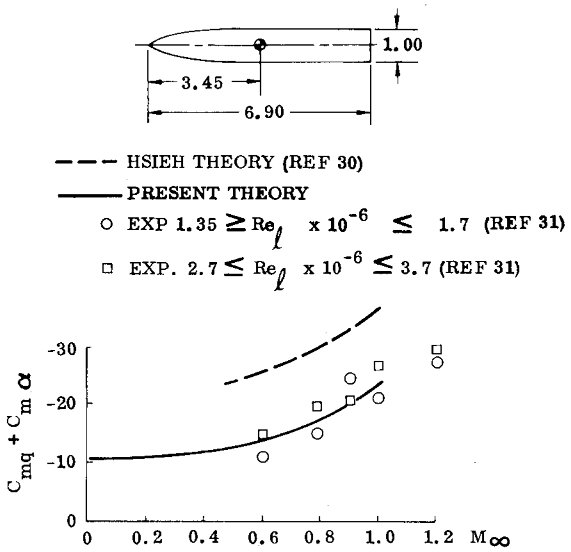

Fig. 12 Predicted and measured pitch damping for an ogive-cylinder body.

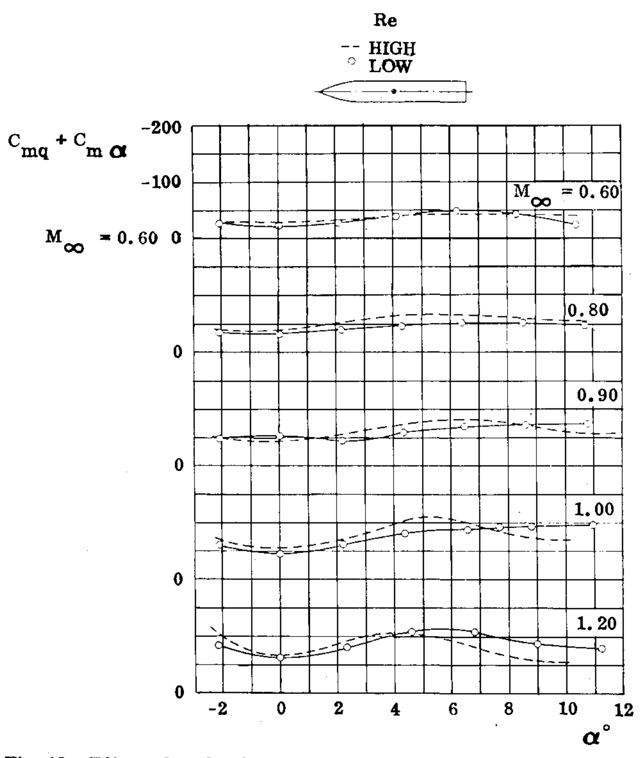

Fig. 13 Effect of angle of attack on the damping of an ogive-cylinder body.[31]

speeds. A similar trend is expected for the loads induced by symmetric vortices. The loads induced by leading edge vortices on slender wings also decrease with increasing (subsonic) Mach number.[6] It can be seen in Fig. 11 that the deviation between experiment and inviscid theory exhibits exactly the data trend expected of vortex-induced loads. As the experiment[28] was performed at $\alpha = 0$ with oscillation amplitudes between 3 and 6 deg, one would not expect bona fide vortex-induced loads to be present. However, viscous crossflow effects similar to those discussed in Ref. 30 are precursory to flow separation with associated symmetric vortex shedding and should, therefore, show the same dependence on Mach number and body slenderness. Furthermore, such pseudo-separation effects are dynamically stabilizing[30] and could, consequently, explain the experimental data trend in Fig. 11.

Results for a long ogive-cylinder are shown in Fig. 12. The agreement with experimental data[31] is better for the present theory than for the more complicated theory of Ref. 32. It can be noted that no subsonic Mach number trend, such as was exhibited in Fig. 11, is detectable in the experimental data in Fig. 12. Although the less slender body geometry could be partially responsible for this difference, the main reason is simply that the test was performed with amplitudes below 3 deg. The pseudo-separation effects[30] become large only just prior to flow separation. Thus, the effects are practically negligible at the small flow inclinations of this test.[32]

At higher angles of attack and/or larger oscillation amplitudes, the viscous crossflow effects have to be included. However, as long as the flow inclinations are well below those causing flow separation, the viscous effects can probably be neglected. According to a recent review of experimental data,[33] the symmetric vortex shedding on ogive- and cone-cylinders will start when the effective flow inclination is in the region $1.2/(l/c) < \alpha < 2.1/(l/c)$, or between $\alpha = 10$ and 18 deg for the body in Fig. 12. Well below this angle of attack, the viscous crossflow effects are assumed to be negligible in the present analysis. The α-characteristics for the body in Fig. 12 support this assumption (Ref. 31 and Fig. 13).

Conclusions

An analysis of slender vehicle dynamics has given the following results:

1) The Newtonian sharp-cone characteristics can be modified to agree with Method of Characteristics computations by accounting for the specific heat-ratio deviation from unity. This modified Newtonian theory can be used with sufficient accuracy down to a moderately low supersonic Mach number determined by the nose slenderness.

2) Combining this γ-corrected Newtonian theory with previously developed analytic means to account for the effect of nose bluntness provides the capability to compute the vehicle dynamics of slender blunted cones at supersonic and hypersonic speeds.

3) For subsonic speeds, a modification of slender-body theory provides simple analytic means for prediction of pointed and blunted slender vehicle dynamics.

4) The end points of the supersonic and subsonic predictions are connected by a straight line fairing.

5) The slender vehicle dynamics computed by the present analytic method agree well with experimental results and with the predictions by other more complicated theories.

Acknowledgments

This paper is based upon results obtained in a study performed for NSWC, Dahlgren, Va., under Contract No. N60921-77C-A294, with J.N.M.N. Sun serving as the program coordinator.

References

[1] Ericsson, L.E., "Modification of Aerodynamic Predictions of the Longitudinal Dynamics of Tactical Weapons," Lockheed Missiles & Space Co., Inc., Sunnyvale, Calif., LMSC-D646354, Contract N60921-77C-A294, Dec. 1979.

[2] Moore, F.G. and Swanson, R.C., Jr., "Aerodynamics of Tactical Weapons to Mach Number 3 and Angle of Attack 15°, Part I—Theory and Application," NSWC/DLTR-3584, Feb. 1977.

[3] Ericsson, L.E., "Unsteady Embedded Newtonian Flow," *Astronautica Acta*, Vol. 18, Nov. 1973, pp. 309-330.

[4] Ericsson, L.E., "Generalized Unsteady Embedded Newtonian Flow," *Journal of Spacecraft and Rockets*, Vol. 12, No. 12, Dec. 1975, pp. 718-726.

[5] Ericsson, L.E., "Viscous and Elastic Perturbation Effects on Hypersonic Unsteady Airfoil Aerodynamics," *AIAA Journal*, Vol. 15, No. 10, Oct. 1977, pp. 481-490.

[6] Ericsson, L.E. and Reding, J.P., "Effect of Angle of Attack and Mach Number on Slender Wing Aerodynamics," *Journal of Aircraft*, Vol. 15, No. 6, June 1978, pp. 358-365.

[7] Ericsson, L.E. and Reding, J.P., "Approximate Nonlinear Slender Wing Aerodynamics," *Journal of Aircraft*, Vol. 14, No. 12, Dec. 1977, pp. 1197-1204.

[8] Ericsson, L.E. and Reding, J.P., "Transonic Sting Interference," *Journal of Spacecraft and Rockets*, Vol. 17, March-April 1979, pp. 140-144.

[9] Bisplinghoff, R.L., Ashley, H., and Halfman, R.L., *Aeroelasticity*, Addison-Wesley, Cambridge, Mass., 1955.

[10] Hayes, W.D. and Probstein, R.F., *Hypersonic Flow Theory*, Academic Press, New York and London, 1959.

[11] Brong, E.A., "The Unsteady Flow Field About a Right Circular Cone in Unsteady Flight," FDL-TDR-64-148, Jan. 1967.

[12] Sims, J.L., "Tables for Supersonic Flow Around Right Circular Cones at Zero Angle of Attack," NASA SP-3004, 1964.

[13] Jones, R.T., "Properties of Low-Aspect-Ratio Pointed Wings at Speed of Sound," NASA Report 835, 1945.

[14] Staff, Aeroballistics Division, NASA MSFC, "Aerodynamic Characteristics of Spherically Blunted Cones at Mach Numbers from 0.5 to 5.0," Huntsville, Ala., MTP-AERO-61-38, May 1962.

[15] Wehrend, W.R., Jr. and Reese, D.E., Jr., "Wind Tunnel Tests of the Static and Dynamics Stability Characteristics of Four Ballistic Re-entry Bodies," NASA TM X-369, June 1960.

[16] Kelly, T.C., "Investigation at Transonic Mach Numbers of the Effects of Configurational Geometry on Surface Pressure Distributions for a Simulated Launch Vehicle," NASA TM X-845, Aug. 1963.

[17] Henderson, W.P., "Pressure Distributions Over the Forward Portion of the Project Fire Space Vehicle Configuration at Mach Numbers from 0.25 to 0.60," NASA TN D-1612, Feb. 1963.

[18] Platzer, M.F. and Hoffman, G.H., "On the Calculation of Dynamic Stability Derivatives for Pointed Bodies of Revolution in Supersonic Flow," Paper 8, *Transactions of the Second Technical Workshop on Dynamic Stability Testing*, Tullahoma, Tenn., Vol. I, April 21-23, 1965.

[19] Lott, R.R., "Evaluation of the Rotational Damping Derivatives for Bodies of Revolution," Revision A, Lockheed Missiles & Space Corp., LMSC-HREC D162655-A, Contract NAS 8-20082, Huntsville, Ala., July 1971.

[20] Chrusciel, G.T., "Aerodynamic Design Parameters for an Advanced Re-entry Vehicle," Lockheed Missiles & Space Corp., Sunnyvale, Calif., IDC 55-21-782, June 21, 1966.

[21] Tobak, M. and Wehrend, W.R., "Stability Derivatives of Cones at Supersonic Speeds," NACA TN 3788, Sept. 1956.

[22] Jaffe, P. and Prislin, R.H., "Effect of Boundary-Layer Transition on Dynamic Stability," *Journal of Spacecraft and Rockets*, Vol. 3, No. 1, Jan. 1966, pp. 46-52.

[23] Wehrend, W.R., Jr., "An Experimental Evaluation of Aerodynamic Damping Moments of Cones with Different Centers of Rotation," NASA TN D-1768, March 1963.

[24] Svendsen, H.O., "An Investigation of the Static and Dynamic Stability of Several Re-entry Body Shapes (R-144)," TM 55-21-78, LMSC-1806311, Jan. 1967.

[25] Uselton, B.L. and Shadow, T.O., "Dynamic Stability Characteristics of 3- and 5- Cal Army-Navy Spinner Projectiles at Mach Numbers 0.2 through 1.3," AEDC-TR-70-115, July 1970.

[26] Ericsson, L.E., "Loads Induced by Terminal-Shock Boundary-Layer Interaction on Cone-Cylinder Bodies," *Journal of Spacecraft and Rockets*, Vol. 7, No. 9, Sept. 1970, pp. 1106-1112.

[27] Ericsson, L.E., "Aeroelastic Instability Caused by Slender Payloads," *Journal of Spacecraft and Rockets*, Vol. 4 No. 1, Jan. 1967, pp. 65-73.

[28] Bykov, V.S., "Calculation of the Characteristics of Aerodynamic Damping of Bodies of Revolution," FTD-HT-23-1363-74, June 1974.

[29] Ericsson, L.E. and Reding, J.P., "Vortex-Induced Asymmetric Loads in 2-D and 3-D Flows," AIAA Paper 80-0191, Jan. 1980.

[30] Ericsson, L.E., "Nonlinear Hypersonic Viscous Crossflow Effects on Slender Vehicle Dynamics," *AIAA Journal*, Vol. 17, No. 6, June 1979, pp. 586-593.

[31] Shadow, T.O., "Investigation of the Half-Model Reflection-Plane Technique for Dynamic Stability Testing at Transonic Mach Numbers," AEDC-TR-76-165, Jan. 1977.

[32] Hsieh, T., "Unsteady Transonic Flow Over Blunt and Pointed Bodies of Revolution," AIAA Paper 78-211, Jan. 1978.

[33] Chapman, G.T. and Keener, E.R., "The Aerodynamics of Bodies of Revolution at Angles-of-Attack to 90°," AIAA Paper 79-0023, Jan. 1979.